ISSN 0208-7774 TRIBOLOGIA 2/2018 p. 21–28

Wacław GAWĘDZKI[*], Dariusz LEPIARCZYK[**], Jerzy TARNOWSKI[**]

A STUDY OF THE IMPACT OF DYNAMIC GROUND ACTIONS ON MOMENTARY VALUES OF FRICTION FORCES AT THE GAS PIPELINE-BACKFILL INTERFACE

BADANIA WPŁYWU ODDZIAŁYWAŃ DYNAMICZNYCH PODŁOŻA NA CHWILOWE WARTOŚCI SIŁ TARCIA W SKOJARZENIU GAZOCIĄG-OBSYPKA

Key words: gas pipeline, friction force, vibration, STFT transformation.

Abstract

Buried pipelines are subjected to the action of static forces and moments caused by friction forces at the pipeline-ground contact. At the same time, pipelines are subjected to dynamic actions generated by paraseismic pulses, in particular, in areas of mining and heavy traffic. The paper presents and experimentally verifies a test method of tribological pipeline-soil interaction in conditions of artificially induced soil static and dynamic actions. The applied test methodology allows the determination of friction forces at the tested pipeline section. The friction forces changes over time on the pipeline and soil surface for the varying pipeline tensioning forces were continuously recorded during the tests. Based on the Short-Time Fourier Transform (STFT) of signals, the paper presents the impact of dynamic actions on momentary values of measured friction forces. Relationships are given that allow the determination of friction forces between the pipeline and the soil, including their limit values resulting in the loss of the mutual adhesion of the pipeline and the soil.

Słowa kluczowe: gazociąg, siła tarcia, drgania, transformacja Fouriera STFT.

Streszczenie

Gazociągi zagłębione w gruncie narażone są na oddziaływania statycznych sił i momentów powstających pod wpływem działania sił tarcia w kontakcie rury z gruntem. Jednocześnie gazociągi poddawane są oddziaływaniom dynamicznym, mającym genezę w impulsach pochodzenia parasejsmicznego. Szczególnie dotyczy to obszarów objętych działalnością górniczą i wzmożonym oddziaływaniem komunikacyjnym. W artykule przedstawiono oraz eksperymentalnie zweryfikowano metodę badań tribologicznej współpracy gazociągu z gruntem w warunkach wywoływanych sztucznie oddziaływań statycznych oraz dynamicznych gruntu. Zastosowana metodyka badawcza pozwala na wyznaczenie wartości sił tarcia na badanym odcinku gazociągu. Podczas badań prowadzono ciągłą rejestrację czasowych zmian sił tarcia na powierzchni gazociągu i gruntu dla zmiennych wartości sił naciągu rury. W artykule, w oparciu o metodę krótkoczasowej transformacji Fouriera (STFT) sygnałów, przedstawiono wpływ wymuszeń dynamicznych na chwilowe wartości mierzonych sił tarcia. Podano zależności umożliwiające wyznaczenie wartości sił tarcia gazociągu i gruntu, w tym także ich granicznych wartości, po przekroczeniu których następuje utrata wzajemnej przyczepności rury i gruntu.

INTRODUCTION

Safety evaluation of gas pipelines located in unstable subsoil (e.g., mining areas, heavy traffic areas) is necessary from the point of view of their use [**L. 1–8**]. Depending on the source, pipelines can be subjected, permanently or periodically, to internal loads (medium pressure and temperature) and external loads (soil weight, overburden load) and, in unstable subsoil, also to quasi-static and dynamic loads caused by the soil deformation [**L. 9**].

The external pipeline loads are caused by quasi-static forces and moments generated by the action of friction forces on the pipeline-subsoil interface and by

[*] AGH University of Science and Technology, Department of Measurement and Electronics, al. A. Mickiewicza 30, 30-059 Krakow, e-mail: waga@agh.edu.pl.

[**] AGH University of Science and Technology, Department of Machinery Construction and Operation, al. A. Mickiewicza 30, 30-059 Krakow, e-mail: ledar@agh.edu.pl, tarnow@agh.edu.pl.

dynamic forces and moments generated by dynamic pulses of paraseismic origin. Vibration caused by shocks and transmitted to the subsoil and pipeline changes friction forces, causing variability of external structure loads. The resonance properties of systems also affect the energy transmission to pipelines by amplification or attenuation of harmful effects of paraseismic actions. The research results in this area that included an analysis of pipeline vibration caused by dynamic actions with the use of Hilbert-Huang Transform HHT and HVD can be found [**L. 10, 11**].

The goal of the experiments presented in this paper was to determine the impact of dynamic subsoil actions on friction forces in the pipeline-soil interface with simultaneous action of static forces. The experiments were conducted on a pipeline section laid in soil in a quartz sand backfill. The dynamic loads in the experiments were artificially triggered soil vibration of a pulse character, which can be interpreted as paraseismic waves generated by mining quakes. Variable values of stabilized static loads on the selected pipeline section were generated by an actuator that could apply the action of different tension forces along the pipeline longitudinal axis. The experiments were conducted in repeatable conditions of the application of static and dynamic actions, ensuring the invariability of parameters and soil mechanical properties. The values of variables acting on the pipeline were measured with the strain gauge technique and recorded during the experiment.

The recorded signals of forces acting on the pipeline section were analysed based on the STFT (Short-Time Fourier Transform). The phenomena occurring at the pipeline-soil interface are non-stationary. Therefore, the application of STFT allows the determination of the friction force signals' frequency spectrum variability in time. These values were determined for various pipeline static tensioning forces and for various intensities of dynamic soil actions. The relationship between the pipeline-quartz backfill friction forces and the values of soil dynamic action in the presence of static pipeline tensioning was proved.

FIELD PIPELINE TESTING FACILITY

Figure 1 presents a diagram of the field pipeline testing facility. The facility was constructed using a section of closed pipeline, 28 m in length and 50 mm in diameter, buried in soil 0.8 m deep in a quartz sand backfill.

Strain gauge transducers for force measurements were installed in places S1 and S2 on the pipeline. The force transducers were implemented using two 0.5 m pipe sections with identical parameters of the tested pipeline. The pipe sections welded into the pipeline were used as elastic converters of force into strain. The axial strain was measured with strain gauge sensors glued onto each pipe section and bridged in a manner compensating the impact of strain caused by bending moments and temperature changes [**L. 9, 12, 13**]. Then, each sensor was calibrated in the laboratory and welded into the suitable placed of the tested pipeline at the test facility (at points S_1 and S_2 – **Fig. 1**).

Measuring points S_1 and S_2 were placed in areas of different pipeline activity. Point S_2 is located between the buried pipe fragments where variations of pipeline-sand backfill friction forces will affect the pipeline activity. On the other hand, point S_1 is located in the beginning of the pipeline, in the direct vicinity of the beginning of the tested pipeline section anchored to soil by means of bolts. Therefore, the impact of the pipeline-backfill friction forces on the pipeline activity will be limited in this point. Dynamic pulses were generated by dropping a 1200 kg weight from approximately 2.7 m at points of dynamic action. **Figure 1** presents points P_1 – P_5 where paraseismic pulses were applied.

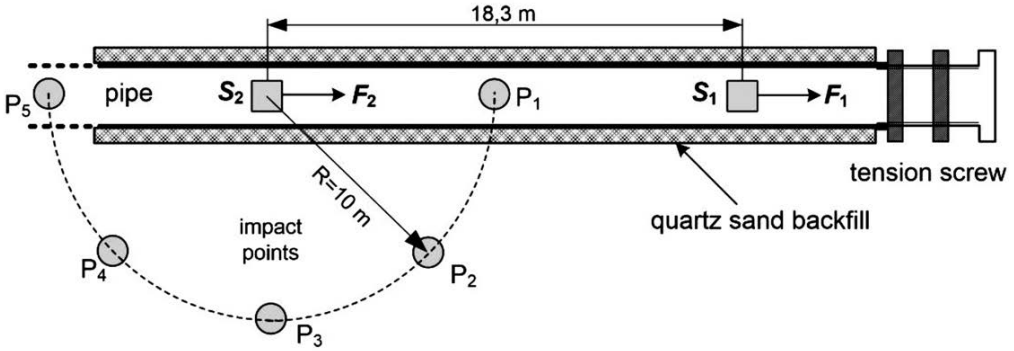

Fig. 1. Diagram of facility to test the impact of static and dynamic actions on pipeline-subsoil friction forces – top view

Rys. 1. Schemat stanowiska terenowego do badań wpływu oddziaływań statycznych i dynamicznych na siły tarcia gazociągu i podłoża – widok z góry

THEORETICAL FOUNDATIONS OF RESEARCH PROCEDURE

The resultant friction force $F_f(t)$ in the 18.3 m section between points S_1 and S_2 is equal to [**L. 8, 9, 11–13**]:

$$F_f(t) = F_1(t) - F_2(t) \tag{1}$$

where

$F_f(t)$ – resultant friction force between pipeline and soil in section between points S_1 and S_2,

$F_1(t)$, $F_2(t)$ – forces acting along the pipeline axis, at points S_1 and S_2 that can be determined based on strains $\varepsilon_1(t)$, $\varepsilon_2(t)$ for the elastic range of pipe behaviour:

$$F_1(t) = A \cdot E \cdot \varepsilon_1(t), \qquad F_2(t) = A \cdot E \cdot \varepsilon_2(t) \tag{2}$$

where

$\varepsilon_1(t)$, $\varepsilon_2(t)$ – measured strain caused by force acting along the pipeline axis at points S_1 and S_2,

A – pipe cross section area,

E – Young's modulus of the pipe material.

Based on (1) and (2), the resultant friction force at the tested pipeline section can be determined from the following relationship:

$$F_f(t) = A \cdot E \cdot [\varepsilon_1(t) - \varepsilon_2(t)] \tag{3}$$

Taking into account the force transducers sensitivity determined during the calibration process, the friction force is

$$F_f(t) = 152{,}6\,\frac{\text{kN}}{‰} \cdot [\varepsilon_1(t) - \varepsilon_2(t)] \tag{4}$$

By means of a tension screw (**Fig. 1**), various values of static pipeline tensioning force F_1 were applied, also changing the pipeline-backfill friction forces in the process. The resultant friction force is the sum of two components: the static friction force F_{fs}, and the dynamic friction force $F_{fd}(t)$:

$$F_f(t) = F_{fs} + F_{fd}(t) \tag{5}$$

where

F_{fs} – static friction force component along the tested pipeline section, between points S_1 and S_2 (**Fig. 1**),

$F_{fd}(t)$ – dynamic friction force component along the tested pipeline section, between points S_1 and S_2.

Mean static friction force on the tested pipeline section, between points S_1 and S_2, during the test time T is

$$F_{fs} = \frac{1}{T}\int_0^T F_f(t)dt \tag{6}$$

where

T – measuring sequence duration.

The dynamic friction force component can be calculated based on (5) and (6):

$$F_{fd}(t) = F_f(t) - \frac{1}{T}\int_0^T F_f(t)dt \tag{7}$$

The maximum value of dynamic friction force component is

$$F_{fd,max} = \max_t \left|F_{fd}(t)\right| \tag{8}$$

Dynamic friction force components $F_{fd}(t)$ have various values depending on static pipe tensioning forces and different intensities of soil dynamic actions. The phenomena occurring at the pipeline-soil interface are non-stationary. Therefore, the recorded dynamic signals of friction forces $F_{fd}(t)$ acting on the pipeline section must be subjected to the time and frequency analysis using the STFT (Short-Time Fourier Transform).

The STFT allows determining the distribution of sinusoidal amplitudes of signal components for frequency values occurring in the analysed signal. It can be used to identify the resonance properties of mechanical systems. The STFT also allows obtaining information on phase relationships between individual components, which can be used in system diagnostics. However, the most important information obtained as a result of the STFT is the determination of frequencies and amplitudes of sinusoidal components occurring in a signal that described non-stationary phenomena.

The application of STFT allows determining the time variability of complex frequency spectrum $SF_{fd}(f,t)$ of friction force signals:

$$SF_{fd}(f,t) = \text{STFT}\left\{F_{fd}(t)\right\} \tag{9}$$

The transform modulus $|SF_{fd}(f,t)|$ is an amplitude frequency spectrum that reaches its maximum $SF_{fd,\max}$ for the following arguments:

$$(f_{max}, t_{max}) = \arg\max\left|SF_{fd}(f,t)\right| \tag{10}$$

and is

$$SF_{fd,max} = \max_f \max_t \left|SF_{fd}(f,t)\right| = \left|SF_{fd}(f_{max}, t_{max})\right| \tag{11}$$

Because the graphical representation of spectrum $|SF_{fd}(f,t)|$, which is a function of two parameters, requires the use of a three-dimensional space, two-dimensional cross sections are often used, allowing, for example, a representation of a sectional view of three-dimensional characteristics of transform $|SF_{fd}(f,t)|$ as a function

of frequency for specified time $t = t_{max}$ for which the characteristics includes the maximum value $SF_{fd,max}$ (9):

$$\left|SF_{fd}(f, t_{max})\right| = \left|SF_{fd}(f, t)\right|_{t=t_{max}} \quad (12)$$

This is a method to obtain an amplitude frequency spectrum for a specific moment of its occurrence.

MEASURING SYSTEM

The measuring system was built based on an 8-channel Spider8 measuring amplifier from Hottinger Baldwin Messtechnik [**L. 14**] connected to a computer by means of an USB interface. The amplifier has measuring channels that allow the integration of strain gauge sensors in bridge systems in the full and half-bridge configurations. Each channel has its own A/D converter and antialiasing filter.

The system was used to measure the pipe longitudinal strain at points P_1 and P_2 with strain gauge sensors in the full bridge configuration, with a 0.5% measurement uncertainty determined by the scaling accuracy. The method of gluing the strain gauge sensors on the measurement section and the arrangement in which they were connected allowed a compensation of non-measured forces' components and moments, and the temperature. The measurement signals were recorded by means of measuring channels and the Spider8 amplifier with a 0.1% measurement uncertainty. The sampling frequency was fs = 1200 Hz, the limit frequency of the antialiasing filter was 150 Hz, and the single recording time was T = 3.33 s.

EXPERIMENTS AND RESULTS

The field testing facility presented in **Figure 1** was used to conduct experiments in conditions of static and dynamic forced. The experiments were conducted for four different nominal values of pipeline tensioning force F_1: 0 kN, 20 kN, 95 kN, and 120 kN. Dynamic pulse actions generated by a falling weight were applied at points P_1–P_5 for each force value (**Fig. 1**). The pipeline longitudinal strain signals $\varepsilon_1(t)$ and $\varepsilon_2(t)$ were recorded at points S_1 and S_2. The strain signals, according to (3), were used to determine friction force $F_f(t)$ at the tested pipeline section between points S_1 and S_2.

Application of dynamic forces at points P_1–P_5 allowed changing the intensity of dynamic soil action on the tested pipeline section, because the distance between the force application point and the pipeline changed. The mean static friction force component F_{fs} was changed by altering of the static pipeline tensioning force.

Figures 2 and **3** present the measurement results for a typical experiment. The figures include curves of tensioning forces $F_1(t)$ and $F_2(t)$, at points S_1 and S_2, respectively. The nominal tensioning force at point S_1 was F_1 = 95 kN (the actual tensioning force F_1 for this experiment was 94.7 kN).

The measured tensioning forces $F_1(t)$ and $F_2(t)$ were used to determine the friction force component $F_f(t)$ according to (4), and the static friction force component F_{fs} according to (6) and the dynamic friction force component $F_{fd}(t)$ according to (7). All determined force vs. time graphs, friction forces, and their components are shown in **Figures 4** and **5**. In addition, **Figure 4** presents the static friction component F_{fs}, and **Figure 5** the maximum value of the dynamic friction force component $F_{fd,max}$.

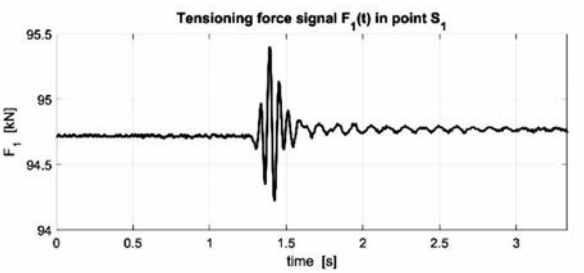

Fig. 2. Tensioning force $F_1(t)$ at point S_1 determined according to (2)

Rys. 2. Przykładowy przebieg siły naciągu $F_1(t)$ w punkcie S_1 wyznaczonej zgodnie z (2)

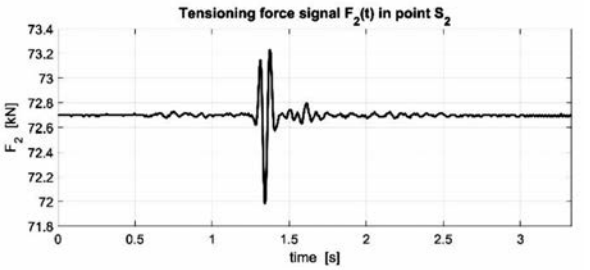

Fig. 3. Tensioning force $F_2(t)$ at point S_2 determined according to (2)

Rys. 3. Przykładowy przebieg siły naciągu $F_2(t)$ w punkcie S_2 wyznaczonej zgodnie z (2)

The STFT (9) was determined for dynamic friction force components $F_{fd}(t)$. The transforms were calculated for recorded 3.3 s signal sequences. Hence, the transform frequency resolution was Δf =1/3.3 s = 0.3 Hz. The *spectrogram* STFT determination algorithm available in Matlab&Simulink calculation environment was used.

Figure 6 shows the STFT-determined amplitude spectrum $|SF_{fd}(f,t)|$ of a friction force signal $F_{fd}(t)$ according to (9). According to (10), the values of variables (fmax,tmax) are determined by the coordinates of the maximum value of amplitude spectrum $SF_{fd,max}$ (11). **Figure 7** presents a sectional view of transform modulus $|SF_{fd}(f,t)|$ as a function of frequency, for specified time $t = t_{max}$ for which the characteristics includes the maximum value $SF_{fd,max}$.

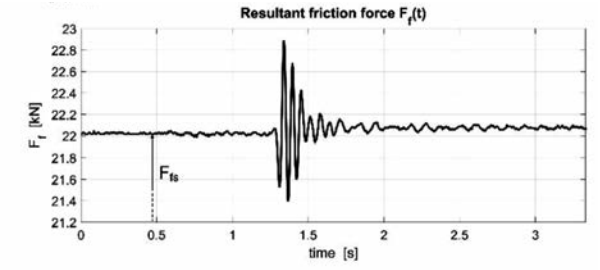

Fig. 4. Resultant friction force $F_f(t)$ determined according to (4), F_{fs} according to (6)

Rys. 4. Przykładowy przebieg wypadkowej siły tarcia $F_f(t)$ wyznaczony zgodnie z (4), F_{fs} zgodnie z (6)

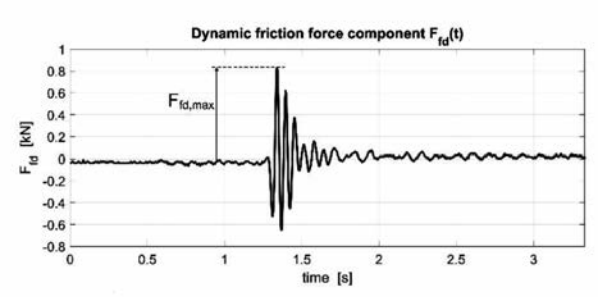

Fig. 5. Dynamic friction force component $F_{fd}(t)$ according to (7)

Rys. 5. Przykładowy przebieg składowej dynamicznej siły tarcia $F_{fd}(t)$ zgodnie z (7)

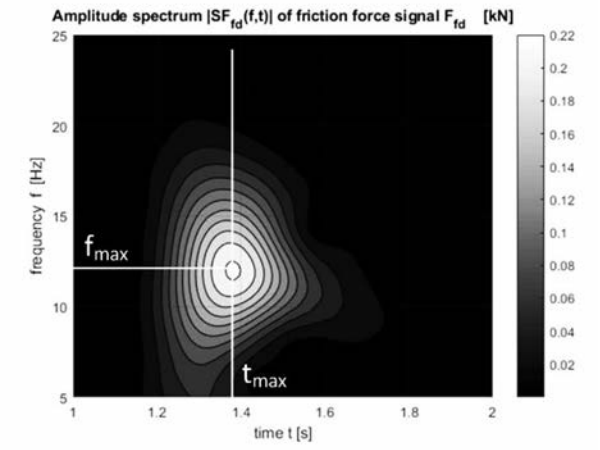

Fig. 6. Amplitude spectrum $|SF_{fd}(f,t)|$ of friction force signal $F_{fd}(t)$ according to (9)

Rys. 6. Widmo amplitudowe $|SF_{fd}(f,t)|$ sygnału siły tarcia $F_{fd}(t)$ zgodnie z (9)

The experiments were conducted at 5 points of application of dynamic pulses (**Fig. 1**), and at each point there were 4 different values of static tensioning force F_1: 0 kN, 20 kN, 95 kN, and 120 kN. There were 20 experiments altogether, and each of them was repeated 5 times to obtain mean values. **Figures 8–11** present families of characteristics for individual points P_1–P_5

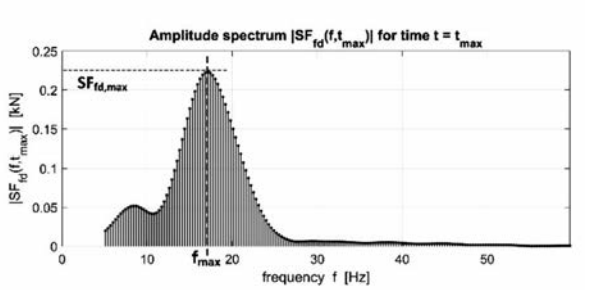

Fig. 7. Amplitude spectrum $|SF_{fd}(f,t_{max})|$ as a function of frequency, for specified time $t = t_{max}$, according to (12)

Rys. 7. Widmo amplitudowe $|SF_{fd}(f,t_{max})|$ w funkcji częstotliwości, dla ustalonego czasu $t = t_{max}$, zgodnie z (12)

of the application of dynamic pulses as a function of static tensioning force F_1 for the following determine magnitudes:

– The static friction force component F_{fs} according to (6) – **Figure 8**,

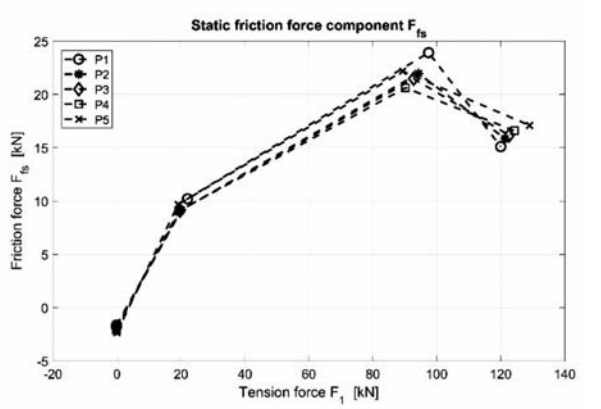

Fig. 8. Static friction force component F_{fs} (according to (6)) as a function of force F_1 for points P_1–P_5

Rys. 8. Statyczna składowa siły tarcia F_{fs} (zgodnie z (6)) w funkcji siły F_1 dla punktów P_1–P_5

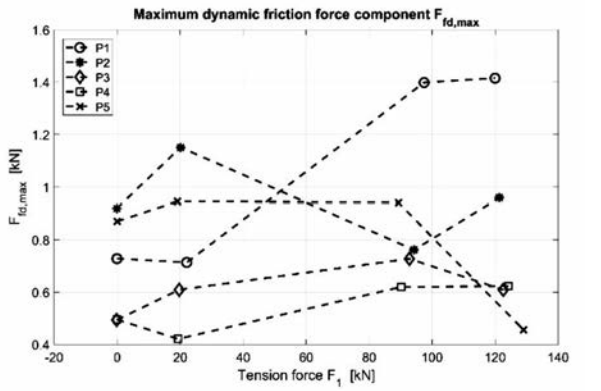

Fig. 9. Maximum dynamic friction force component $F_{fd,max}$ (according to (8)) as a function of force F_1 for points P_1–P_5

Rys. 9. Maksymalna wartość składowej siły tarcia $F_{fd,max}$ (zgodnie z (8)) w funkcji siły F_1 dla punktów P_1–P_5

– The maximum dynamic friction force component $F_{fd,\max}$ according to (8) – **Figure 9**,
– The maximum dominating component in the spectrum $SF_{fd,\max}$ according to (11) – **Figure 10**, and
– The resonance frequency $f_{\max}$ according to (10) – **Figure 11**.

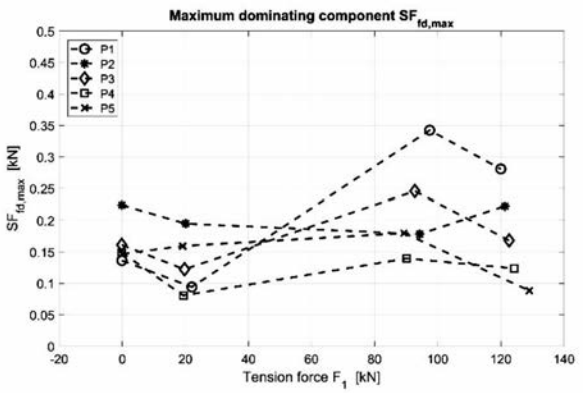

Fig. 10. Maximum dominating component $SF_{fd,\max}$ (according to (11)) as a function of force F_1 for points P_1–P_5

Rys. 10. Maksymalna wartość składowej dominującej $SF_{fd,\max}$ (zgodnie z (11)) w funkcji siły F_1 dla punktów P_1–P_5

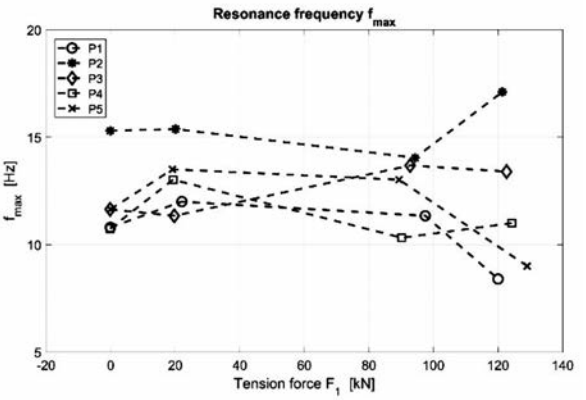

Fig. 11. Resonance frequency fmax (according to (10)) as a function of force F_1 for points P_1–P_5

Rys. 11. Częstotliwość rezonansowa fmax (zgodnie z (10)) w funkcji siły F_1 dla punktów P_1–P_5

ANALYSIS OF RESULTS

Let us consider force vs. time graphs $F_1(t)$, $F_2(t)$, $F_f(t)$, and $F_{fd}(t)$ shown in **Figures 2** through **5**. They are from the experiment in which the dynamic pulse was applied at point P_2, and the tensioning force values were F_1 = 94.7 kN and F_2 =72.7 kN, respectively. According to (1), the friction force static component on the tested section, between points S_1 and S_2, was F_{fs} = 22 kN. The friction force dynamic component $F_{fd}(t)$ presented in **Figure 5** reaches $F_{fd,\max} \cong 0.82$ kN, which is 3.7% of the friction force static component.

Let us also consider cumulative graphs in **Figures 8** and **9** which comprise all measurement points. The analysis of the graphs indicates that, for instance, at measuring point P_1 for the tensioning force F_1 = 97 kN, the friction force dynamic component $F_{fd}(t)$ reaches 1.4 kN (**Fig. 9**), which is almost 6% of the friction force static component which equals F_{fs} = 24 kN (**Fig. 8**). This means that, as a result of dynamic pulses with energy values that occur in practical conditions, the resultant friction force on the pipeline-quartz sand backfill interface can vary by at least ±6% (value verified by measurements) relative to the static friction force.

Figure 8 also indicates that, regardless of the action application point P_1–P_5, the friction force static component F_{fs} has practically the same values which depend only on the static tensioning force F_1 (the graphs practically coincide). In addition, it can be stated that, when the static tensioning force increases, the friction force static component F_{fs} (**Fig. 8**) initially grows, and then, after exceeding of a certain F_1 value, it begins to drop.

Using the STFT, let us determine the frequency values of sinusoidal components occurring in the signal and their amplitudes. **Figure 6** shows, for the case discussed above, the amplitude spectrum $|SF_{fd}(f,t)|$ of the friction force signal $F_{fd}(t)$ according to (9). The figure includes the maximum value which occurs for frequency fmax at time tmax. **Figure 7** shows a sectional view of the spectrogram from **Figure 6** with amplitude spectrum $|SFfd(f,t_{\max})|$ as a function of frequency for specified time $t = t_{\max}$, according to (12). The maximum value for dominating component of frequency fmax is $SF_{fd,\max} \cong$ 0.22 kN. It is significantly smaller than the above-mentioned maximum value in time domain $F_{fd,\max} \cong$ 0.82 kN (**Fig. 5**), the reason being the fact that a large portion of energy is also distributed on the remaining harmonic components of spectrum $|SF_{fd}(f,t_{\max})|$. Let us also consider cumulative graphs in **Figures 10** and **11**, which include all measurement points. The maximum value of dominating component $SF_{fd,\max}$ (according to (11)) as a function of force F_1 for all points of pulse forcing P_1–P_5 grows along with the increase of the pipeline tensioning force from 20 kN to 95 kN. This means that the increase of static tensioning force F_1 is accompanied not only by the increase of the friction force static component (**Fig. 8**), but also by the increase of the impact of dynamic actions on the value of dominating dynamic friction force component $SF_{fd,\max}$ (similarly as for $F_{fd,\max}$ – **Fig. 9**). However, after a certain value of force F_1 is exceeded, the value of dominating dynamic friction force component $SF_{fd,\max}$ begins to drop (except P_2). This confirms earlier conclusions from the time domain analysis that the pipeline contact with the sand backfill deteriorates due to the friction force decrease.

However, the determination of the STFT most of all allows determining the resonance frequency values fmax (according to (10)) of the dominating dynamic friction force component dominating dynamic friction force component SFfd,max. **Figure 11** presents the resonance frequency graphs fmax as function of force F_1 for all points P_1–P_5 in which pulses were applied. Generally, it can be concluded that the frequency of the dominating component does not significantly depend on the tensioning force F_1 and on the pulse application point P_1–P_5. The resonance frequencies are in the 10––15 Hz for almost all cases. However, their value depends mainly on the condition and quality of the contact at the pipeline-quartz sand backfill interface.

CONCLUSIONS

The goal of the paper was to determine the impact of paraseismic dynamic actions of soil on momentary values of friction forces at the contact of a buried pipeline with a quartz sand backfill. The results of experimental field tests were presented, during which the values of friction forces were determined at the pipeline-backfill interface. The source of pipeline loads were artificially triggered soil vibration of a pulse character. The values of tensioning forces $F_1(t)$ and $F_2(t)$ at places designated S_1 and S_2 were recorded (**Fig. 1**). The recorded tensioning force signals were used to determine the following friction forces and their components: the friction force static component F_{fs}, and the friction force dynamic component $F_{fd}(t)$. The experiments were repeated many times for various points of the application of dynamic actions P_1–P_5, which allowed changing the intensity of dynamic actions on the examined pipeline section, as the distance between the application point and the pipeline changed.

The change of the mean friction force F_{fs} was obtained by changing the pipeline static tensioning force.

The determined friction force components were analyses in the time domain, and the dynamic component $F_{fd}(t)$ was also subjected to the Short-Time Fourier Transform (STFT) dedicated to non-stationary signals. The following conclusions can be formulated based on the analysis of friction force signals with the use of the STFT:

– The maximum value of dominating friction force component SFfd,max as a function of tensioning force F_1 was determined for all points of pulse application P_1–P_5. It was determined that the dominating friction force component grows along with the increase of the pipeline static tensioning force in a certain interval of tensioning forces F_1, and after the exceeding of which the $SF_{fd,\max}$ begins to drop, so it behaves in a similar way to the friction force static component F_{fs}. This confirms earlier conclusions from the time domain analysis that the pipeline contact with the sand backfill deteriorates due to the friction force decrease.
– The occurrence of the resonance of the friction force dynamic component $F_{fd}(t)$ in the pipeline section in full frictional contact with soil was confirmed. The 10–15 Hz resonance frequency range was determined, exempt for single cases. It was determined that the value of resonance frequency depends mainly on the condition and quality of the contact between at the pipeline-quartz sand backfill interface and the impact of the pipeline static tensioning and the intensity of dynamic actions is small.
– The experiments allowed finding the tribological conditions and determining the maximum values of the friction force dynamic component $F_{fd}(t)$ occurring at the contact of the monitored pipeline with the backfill, depending on the friction force static component $F_{fs}(t)$. Both friction force components, occurring in conditions or paraseismic vibration, have a significant impact on the loads of pipelines built in unstable areas.
– The presented measurement methodology of momentary friction force values and their extreme values allow choosing preventive measures to reduce the hazards for pipelines subjected to continuous soil deformation (soil movements) and paraseismic vibration.

The changes of friction force values presented in the paper can be applied at the design stage of pipelines used in similar conditions, and compensators or a constant monitoring can be applied to minimize the impact of such changes on the total pipeline deformation during the construction and the transport of gas.

ACKNOWLEDGEMENTS

This research was financed by resources for statutory activities of the Department of Metrology and Electronics, AGH.

REFERENCES

1. Abdoun T.H., et al.: Factors influencing the behavior of buried pipelines subjected to earthquake faulting. Soil Dynamics and Earthquake Engineering, 29 (3), 2009, pp. 415–427.
2. Chen W.W., et al.: Seismic response of natural gas and water pipelines in the Ji-Ji earthquake. Soil Dynamics and Earthquake Engineering, 22 (9–12), 2012, pp. 1209–1214.

3. Dulińska J., Zięba A.: Wpływ wstrząsów górniczych i odstrzałów w kamieniołomach na odpowiedź dynamiczną gazociągu. Czasopismo Techniczne 2007, Budownictwo z.2-B, s.19–28.
4. Figiel W., Tarnowski J.: Badania współczynnika tarcia rurociągu i gruntu na terenach górniczych w obecności wstrząsów. Eksploatacja i Niezawodność – Maintenance and Reliability, 4, 2005, s. 55–63.
5. Gawędzki W.: Analiza wpływu drgań gruntu na odkształcenia rurociągów w warunkach ich dodatkowego obciążenia statycznego. Pomiary, Automatyka, Kontrola, 56 (8), 2010, s. 879–882.
6. Honegger D.G., Wijewickreme D.: Seismic risk assessment for oil and gas pipelines. In Seismic Risk Analysis and Management of Civil Infrastructure Systems. Woodhead Publishing, Part IV, 2013, pp. 682–715.
7. Kim D.S., Lee J.S.: Propagation and attenuation characteristics of various ground vibrations. Soil Dynamics and Earthquake Engineering, 19, 2000, pp. 115–126.
8. Lepiarczyk D., Gawędzki W., Tarnowski J.: Analysis of the influence of friction force on the strains of gas pipeline using the Hilbert-Huang transform. Tribologia , 4, 2016, pp. 145–155.
9. Gawędzki W., Tarnowski J.: Design and testing of the strain transducer for measuring deformations of pipelines operating in the mining-deformable ground environment. Measurement Science Review, 15 (5), 2015, s. 256–262.
10. Gawędzki W., Serzysko B.: Zastosowanie transformacji Hilbert Vibration Decomposition do analizy sygnałów parasejsmicznych w dziedzinie czasu. Przegląd Elektrotechniczny, 91 (8), 2015, 7–10.
11. Gawędzki W., Tarnowski J.: A study of the influence of friction forces on the transmission of soil vibration on gas pipelines. Tribologia , 2, 2017, pp. 49–58.
12. Hoffmann K.: An Introduction to Measurements using Strain Gages. Publisher Hottinger Baldwin Messtechnik GmbH, Darmstadt 1989.
13. Gawędzki W.: Pomiary elektryczne wielkości nieelektrycznych. Wydawnictwa AGH, Kraków 2010.
14. Hottinger Baldwin Messtechnik, Spider8 amplifier and Catman® software Technical Documentation, http://www.hbm.com.